



# Modeling the spray characteristics of blended fuels for gasoline direct injection applications

Akhil Ailaboina & Kaushik Saha

**To cite this article:** Akhil Ailaboina & Kaushik Saha (2023) Modeling the spray characteristics of blended fuels for gasoline direct injection applications, International Journal of Green Energy, 20:12, 1326-1341, DOI: [10.1080/15435075.2022.2057801](https://doi.org/10.1080/15435075.2022.2057801)

**To link to this article:** <https://doi.org/10.1080/15435075.2022.2057801>



Published online: 06 Apr 2022.



Submit your article to this journal 



Article views: 729



View related articles 



View Crossmark data 



Citing articles: 5 View citing articles 

# Modeling the spray characteristics of blended fuels for gasoline direct injection applications

Akhil Ailaboina and Kaushik Saha

Engines and Unconventional Fuels Laboratory, Department of Energy Science and Engineering, Indian Institute of Technology Delhi, New Delhi, India

## ABSTRACT

Methanol and ethanol are considered as potential candidates for alternative fuels in spark-ignited engines and flex-fuel vehicles. Alcoholic fuels have higher latent heat of vaporization ( $h_{fg}$ ), lower boiling-point temperature and higher-octane numbers help the engine run under higher compression ratios, resulting in better efficiency and fuel economy. A numerical study is carried out to understand the spray-breakup and vaporization characteristics of binary blended fuel and ternary fuel blend compared to single-component fuel for gasoline direct injection (GDI) system. Multiple simulations were carried out by substituting individual fuel properties of iso octane with those of ethanol to understand the relative importance and effect of fuel properties on spray characteristics. The spray characteristics of pure iso octane fuel and their blends with ethanol and methanol are studied and compared, and the charge cooling effects for alcoholic fuels have been observed. The Spray G operating condition has been taken from the Engine Combustion Network (ECN) for this study. The simulated data for iso octane has been validated with the experimental data from the ECN, and a similar model setup has been used for pure and blended fuel sprays. The discrete-phase modeling (DPM) approach is carried out, and the Unsteady Reynolds-Averaged Navier-Stokes (URANS) RNG (Renormalization)  $k-\epsilon$  turbulence model is considered in understanding the spray characterization. The blended methanol fuels have higher penetration lengths compared with ethanol ones. The penetration of the blended fuels (binary and ternary) is slightly lower than the iso octane. The ternary blends showed spray characteristics similar to those of E85, and it indicates that the ternary blended fuel has the potential to be used as a drop-in fuel for a GDI-based flex-fuel vehicle.

## ARTICLE HISTORY

Received 8 November 2021  
Accepted 19 March 2022

## KEYWORDS

Gasoline direct injection (GDI); alternative fuels; blended fuels; spray modeling; flex-fuel vehicles (FFV); drop-in fuels

## 1. Introduction

With an enormous increase in the number of automobiles powered by an internal combustion engine (ICE), the requirement for fuel has also been increasing. However, with their increased use, fossil fuels are depleting at a tremendous pace than expected. Since the sources for extracting petroleum products are very low in a country like India, to meet the needs of the requirement, the majority of the crude oil is being imported (Ministry of Petroleum and Natural Gas Economic & Statistics Division 2022). Due to the market fluctuations around the globe, the price of petroleum-based fuels has been increasing immensely. The other concern to handle is the burning of petroleum products and the air pollution caused by emissions coming from vehicles. Considering the effects of tailpipe emissions and global warming, there is considerable debate in the scientific community as well as various environmental bodies (Govt/NGOs) in the international forums such as COP 26, to ban ICE vehicles (ICEV) and encourage the use of battery electric vehicles (BEV). The scientific community supporting the BEVs was not considering the life-cycle analysis (LCA) of the BEV system and the potential comparison of global warming potential (GWP) with plug-in hybrid electric vehicles (PHEVs) and full hybrid electric vehicles (FHEVs). Table 1 compares 2020 GWP percentage reductions by technology

with estimated 2050 values. Surprisingly, the PHEVs and FHEVs are not far from the BEVs (Publications Office of the EU n.d.) It necessitates the investigation of alternative fuels to reduce the dependency on fossil fuels and tailpipe emissions. Of all the fuels considered as an alternative to gasoline, alcohol fuels are one of India's most promising fuels due to the availability of the feedstocks to produce ethanol and coal reserves to produce methanol. Alcohols offer various advantages as fuel compared to traditional nonrenewable oil resources. Alcohol fuels have high-octane numbers, higher latent heat of vaporization, lower boiling point and higher flame speed, lower sulfur content, and less overall emissions than gasoline (Price et al. 2007). The physical properties of the alcohol fuels are compared with iso octane in Table 2.

The USA's Energy Independence and Security Act of 2007 have proposed using renewable fuels of 36 billion gallons per year in its vehicles by 2022 (H.R.6 - 110th Congress (2007–2008): Energy Independence and Security Act of 2007 | Congress.gov | Library of Congress (2021)). Similarly, European Union (EU) Renewable Energy Directive (RED) has thought to establish the usage of 10% of renewable fuels by 2020 (European Union 2009). Ethanol is the most widely used blended fuel in the USA and Brazil, where 10% of the ethanol blend with gasoline is readily available and called

**Table 1.** Global warming potential (GWP) percentage reductions by technology from the Ricardo (2020) life cycle analysis (LCA) (Adapted from (Senecal and Leach 2021)).

Vehicle type	2020	2050
ICEV (gasoline)	0	-38
ICEV (diesel)	-15	-55
FHEV (gasoline)	-22	-55
FHEV (diesel)	-30	-62
PHEV (gasoline)	-45	-78
PHEV (diesel)	-47	-78
BEV	-53	-84

**Table 2.** Physical properties of isoctane, ethanol, and methanol at standard temperature and pressure (STP) (Yates et al. 2010; Verhelst and Wallner 2009).

Property	Isooctane	Ethanol	Methanol
Stoichiometric AFR (:1)	15.00	9.00	6.46
Density ( $\text{kg}/\text{m}^3$ )	692	789	792
Boiling point at 1 bar ( $^\circ\text{C}$ )	99	77.8	65
Heat of vaporization (kJ/kg)	270	838	1100
Surface tension (20 $^\circ\text{C}$ ) (mN/m)	18.6	22.3	22.1
Dynamic viscosity (20 $^\circ\text{C}$ ) [mPa.s]	0.5	1.2	0.57
Molecular weight (g/mol)	114.23	46	32
Research octane number (RON)	100	108.6	108.7

gasohol. In 2010 the Environmental Protection Agency (EPA) approved 15% of ethanol blend with gasoline, which shows the commitment to reducing fossil fuel dependency. The usage of renewable fuels is not new to society. The scientific community of ICE has been trying to study alternative fuel potential, especially alcoholic fuels, since the early 1980s. In 1992 the USA government authorized the usage of E85 fuel (marketing term for ethanol-gasoline blends containing 51% to 83% ethanol, depending on geography and season) (Alternative Fuels Data Center: Ethanol Benefits and Considerations 2021). Since alcoholic fuels are corrosive, they require special material treatment to avoid adverse results. In the early 1980s, flex-fuel vehicles (FFV) were developed, operating with a wide range of different fuels or fuel blends. These vehicles are mostly run with the blend composition of E85 and below. The ethanol blend with gasoline has reduced particulate emissions because of low carbon content and no aromatic compounds. However, the fuel economy of E85 vehicles has been reduced to 29% compared with the gasoline fuel to ethanol's low energy content (Jin et al. 2017).

Ethanol is the kind of alcohol fuel that has shown promising results in Brazil and the USA regarding flex-fuel vehicles. However, ethanol's manufacturing and processing costs are high, unlike Brazil, which has a better production-to-consumption ratio than others. Most other nations cannot produce ethanol efficiently by the first-generation process, i.e., ethanol is made from biomass feedstocks. This can be overcome by adopting the second-generation processes, allowing a more comprehensive range of feedstocks to produce ethanol (Aditiya et al. 2016). The places where ethanol production is challenging and cost-effective can look into another alternative among the alcohol fuels, such as methanol. For India, methanol is projected to be one of the best alternative fuels. National Institution for Transforming India (NITI Aayog) has also recommended methanol as a futuristic engine fuel in its methanol economy program (Methanol Economy |

NITI Aayog 2021). Methanol can be obtained from coal, natural gas, biomass, wood landfills, etc. Biomass processing is the most cost-effective method for processing methanol (Aditiya et al. 2016; Methanol Economy | NITI Aayog 2021; Verhelst et al. 2019). Additionally, methanol and ethanol are miscible with each other and separately with gasoline too. It can be a promising fuel to mix with binary blends of ethanol and gasoline to reduce ethanol and gasoline utilization in the FFVs. The demand for methanol in the global market has also increased in the last few years. However, there are a few disadvantages of using methanol as a fuel, such as they are corrosive and has a low calorific value (almost half of the gasoline). Combustion of alcohol fuels produces formaldehyde in the exhaust, which is a severe exhaust pollution problem, and it has poor cold-weather starting characteristics (Safe Handling | METHANOL INSTITUTE 2021). These limitations can be reduced by blending alcoholic fuels with gasoline.

As mentioned earlier, the usage of binary blends such as Ethanol-Gasoline and Methanol-Gasoline is accepted worldwide. However, considering the fuel utilization pace, several investigations have been carried out to see the effect of blending gasoline, ethanol, and methanol, all three of them together (Aditiya et al. 2016; Jin et al. 2017; Methanol Economy | NITI Aayog 2021; Safe Handling | METHANOL INSTITUTE 2021; Turner et al. 2011, 2012, 2013; Verhelst et al. 2019). The blending of these fuels in this work will be referred to as GEM, followed by the volume percentage in the mixture (example-G37E21M42). The blend proportions and their physical properties will be explained in the coming section. Experiments were conducted using the GEM fuels on a port fuel injected (PFI) engine (Turner et al. 2013).

Moreover, usage of gasoline direct injection (GDI) systems has been increased widely in the past two decades because of their capability of producing lower exhaust emissions and yielding improved volumetric efficiency (Carsten 2006; Zhao, Lai, and Harrington 1997). The gasoline-type fuel is injected directly into the combustion chamber in GDI systems instead of the intake manifold. The atomization of the fuel spray mainly influences the combustion performance of an ICE. If the atomization of the fuel spray is proper, it leads to faster vaporization and better charge preparation. Therefore, understanding spray characteristics is a prerequisite to developing a better combustion system. Over the past two decades, enormous research has been carried out by several research groups on GDI systems across the globe through numerical and experimental techniques (Allocca et al. 2018; Cordier, Itani, and Bruneaux 2020; Duke et al. 2017a, 2017b; Gutierrez et al. 2018; Liu et al. 2021; Mohapatra et al. 2020; Paredi et al. 2018; Payri et al. 2017; Piazzullo et al. 2017; Yue, Battistoni, and Som 2018). However, there is limited literature on spray studies using GEM fuel on direct injection systems. This is because most of the geometrical specifications of the fuel injectors and the knowledge available of the same are minimal. In this work, the spray simulations using the Spray G injector from the Engine Combustion Network (ECN) are carried out to take advantage of the available geometrical specifications and other parameters of the GDI systems in the ECN database. From the past decade, experimental and numerical investigations on

Spray G injector to obtain a better spray modeling approach and evaluate the spray characteristics have increased immensely from different global research groups. More details and operating conditions of the Spray G injector can be found on the ECN website ('Spray G' Operating Condition – Engine Combustion Network 2021). Moreover, the RNG k- $\epsilon$  turbulence model is rarely used in GDI spray modeling. However, RNG is mostly used when it comes to ICE combustion modeling. Therefore, a validated spray model using RNG k- $\epsilon$  has not been used for blended fuels. The current work addresses that research gap in the literature.

This work is presented in the following way: firstly, model details – details of blends considered in this study, their properties, governing equations, model and sub-models, boundary, and initial conditions. Secondly, model validation and results from parametric studies to understand the spray characteristics of the blends. Finally, the work is concluded with a summary and conclusions.

## 2. Model details

A counter-bored GDI fuel injector with eight holes called Spray G from ECN is considered in this study. ECN is an open-access research database on the spray and combustion of internal combustion engines, involving various research laboratories, industries, and researchers from different universities, across the globe working on IC engines. The Spray G geometry taken from ECN is shown in Figure 1. Geometry details and dimensions are shown in Figure 2. The operating conditions of Spray G are mentioned in Table 3.

This numerical work is carried out by using the computational fluid dynamics (CFD) code CONVERGE v2.4. The conservation equations of mass, momentum, species, energy are solved. The Unsteady Reynolds Averaged Navier-Stokes (URANS) RNG (Renormalization) k- $\epsilon$  turbulence model is considered in this study. A significant number of publications adopt the URANS approach for spray and combustion CFD study (Aguerre and Nigro 2019; Duke et al. 2017b; Han and Reitz 1995; Kim, Song, and Park 2015; Mohapatra et al. 2020; Paredi et al. 2020; Saha et al. 2016, 2017). The transport equations are solved using the PISO (Pressure Implicit with Splitting of Operators) algorithm. Furthermore, the code also solves the sub-models of spray, such as spray breakup, evaporation, collision, and wall interaction. A variable-time step

**Table 3.** Operating conditions of Spray G ('Spray G' Operating Condition – Engine Combustion Network 2021).

Ambient gas temperature	573 K
Ambient gas pressure	6.0 bar (N <sub>2</sub> )
Ambient gas density	3.5 kg/m <sup>3</sup>
Fuel injection pressure	200 bar
Fuel temperature at the nozzle	363 K
Injection mass	10 mg
Injection duration	780 $\mu$ s
Fuel	Isooctane
Orifice diameter	0.165 mm

algorithm is used in this study, in which the timestep is automatically calculated using the maximum allowed CFL (Courant-Friedrichs-Lowy) numbers, spray, and evaporation timestep values. The ROI (Rate of injection) profile, i.e., fuel injection rate vs. time, as shown in Figure 3, is used to initialize the simulation, and the same has been obtained from the ECN database.

Understanding the spray phenomena in a GDI engine is challenging because the engine running conditions are associated with vibrations, and the operations taking place, such as piston movement, intake, and exhaust valve movements during the run time, are complex. Theoretically speaking, combustion in a spark-ignited (SI) engine is approximated as a constant volume heat addition process. Since the spray studies are non-reacting, understanding its characteristics at different operating conditions can be easily mimicked with the help of a constant volume chamber (CVC) without violating the fundamental laws. This work uses a cylindrical domain of dimensions 108 mm diameter and 108 mm length as a computational domain, as shown in Figure 4. The injector tip is located at the center of the domain on the top surface. The blob injection approach is used in this study to distribute the number of droplets, and the injected drop sizes are equal to the nozzle hole diameter (Reitz 1987). The Kelvin-Helmholtz (KH) - Rayleigh-Taylor (RT) breakup length model is used in this study to simulate the breakup of the liquid jet. Two models, such as the O' Rourke numerical scheme and the NTC (No Time Counter) collision method, are available in the code for collision and coalescence. Out of which NTC collision method is used for collision. The reason for it is that this model is faster and more accurate comparatively (Schmidt and Rutland 2000). The Rebound/Slide method is adopted to model the drop and wall interaction. The Frossling correlation model is used for droplet

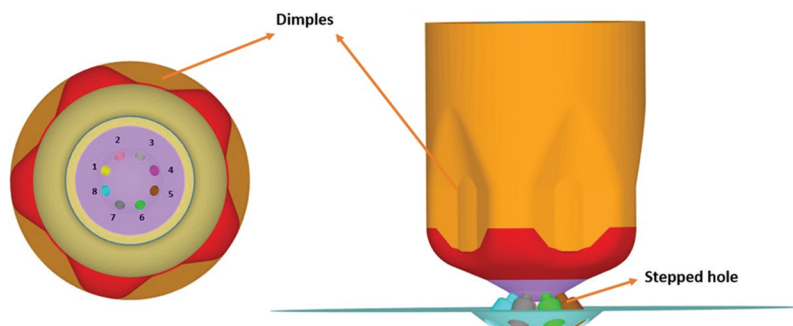


**Figure 1.** The layout of the eight stepped holes of the Spray G nozzle (bottom view and side view)

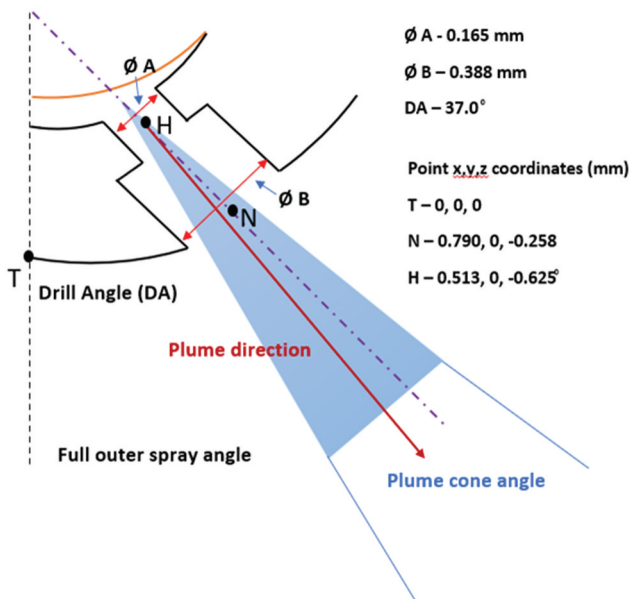


**Figure 2.** Geometry and dimensions of Spray G injector ('Spray G' Operating Condition – Engine Combustion Network 2021)

vaporization. The experimental data of the properties of fuel blends used in this study are not available. Initially, the NIST REFPROP was used to get the fuel properties of the blends since this software is known to be used for such applications. However, while estimating the properties of a binary or ternary blend using the NIST REFPROP (version 10), it has been observed that not all the values of the required properties could be provided by the REFPROP due to some limitations in the algorithms used in the software. Hence a different approach is carried out in this work to vaporize the fuel droplets. The CONVERGE code allows the individual fuel species to vaporize accordingly. The properties of individual fuel species in the liquid phase (e.g., saturation pressure, density, viscosity, latent heat, etc.) are included in the case set up, and those property values are considered during the simulation run-time. More details regarding the governing equations and sub-models can be found here (Richards and Senecal 2021).

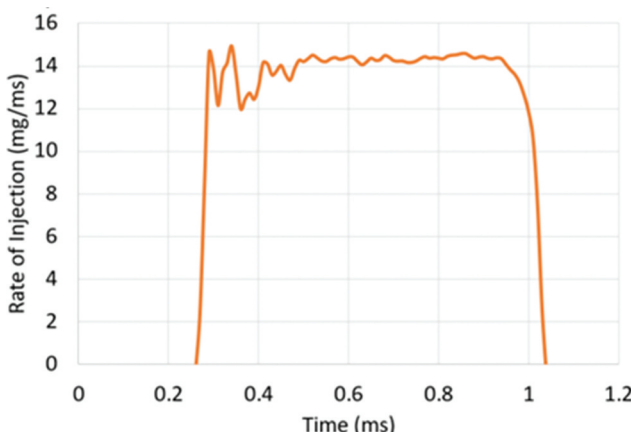


**Figure 3.** Rate of injection profile for Spray G ('Spray G' Operating Condition – Engine Combustion Network 2021).

## 2.1. Ternary blends of gasoline, ethanol, and methanol

To use the ternary blends as drop-in fuels for the E85-based FFV direct-injection spark-ignited engine, it is essential to maintain the same air-fuel ratios (AFRs) as the binary gasoline-ethanol blend (E85), much used in most FFVs. The present study is inspired by the work carried out by Turner et al. (2012), and the same blend configuration has been used in this study. However, it is to be noted that the work carried by Turner et al. (2011, 2012, 2013) is on a PFI engine, and this work is focused on knowing the behavior of the blended fuels at high pressure and temperature seen in a GDI engine.

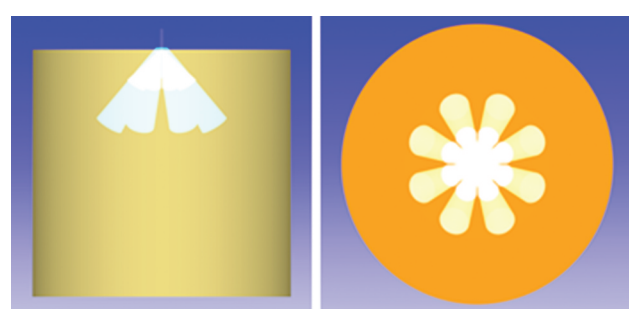
The stoichiometric AFR of E85 is known to 9.74:1. However, it depends on the composition of the gasoline used in the blend. Both ethanol and methanol have a stoichiometric AFR less than the E85 because they are pure components. In order to overcome the effects of various AFRs with change in different gasoline fuel components, isoctane, a surrogate for gasoline, is considered in this study. The comparison of stoichiometric AFR and other parameters of pure components is shown in Table 2.

In this work, five blends were considered, and all are maintained with the stoichiometric AFR of 9.7, equal to that of E85 fuel. The blend properties are shown in Table 4, and the volume relationships between the components are shown in Figure 5. The blends mentioned are used on a production flex-fuel vehicle certified to Euro 5 emission norms. The FFV's exhaust emissions, performance, and economic analysis using the different GEM blends are explained thoroughly here (Turner et al. 2012, 2018). However, it is worth noting that the FFV on which tests were performed is equipped with a port fuel injection system. Specifications of the engine are shown here (Turner et al. 2012, 2013).

Figure 5 mentions each fuel's composition to be maintained to achieve the AFR equivalent to E85 fuel. On the right, at 85% of ethanol, the gasoline composition is 15% to achieve an AFR of 9.7. The same can be obtained with the blend configuration of gasoline at 29.5%, ethanol at 42.5%, and methanol at 28%.

## 3. Results and discussions

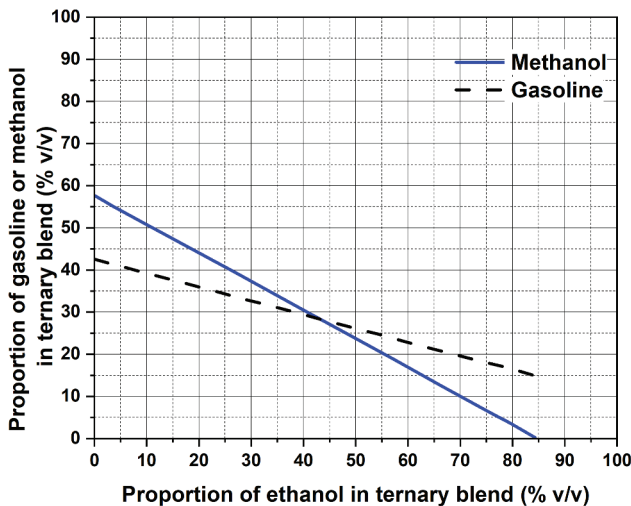
In this section, the results obtained from the numerical simulations are organized as follows: validation of the Spray G computational setup with the experimental data; parametric studies on evaluating the influence of fuel properties; comparison of binary blended fuels with isoctane fuel; and comparison of different GEM blends.



**Figure 4.** Constant volume chamber computational domain with spray embedding (side view and top view).

**Table 4.** Properties of GEM ternary blends used in this work (Adapted from (Turner et al. 2011)).

Properties	G15E85M0	G29.5E42.5M28	G37E21M42	G39E15M46	G40E10M50	G42E5M53
AFR	9.69	9.69	9.71	9.70	9.65	9.67
Density (kg/l)	0.781	0.773	0.769	0.768	0.767	0.766
LHV (MJ/kg)	29.09	29.38	29.56	29.59	29.46	29.56
RON	107.4	107.4	106.4	105.3	105.6	105.6

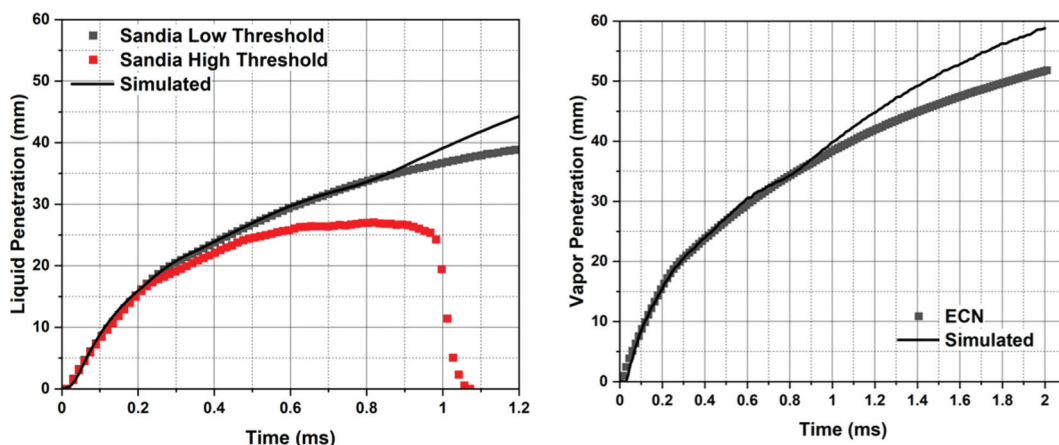
**Figure 5.** Volume % relationship of three components in a GEM blend to maintain AFR similar to that of E85 (Adapted from (Turner et al. 2012)).

### 3.1. Model validation

This work is carried out by using a grid resolution where 1 mm and 0.125 mm are maximum and minimum grid sizes, respectively. The nozzle hole diameter of the Spray G injector is 0.165 mm. Considering the blob injection approach in this study, the maximum diameter of the parcel injected at the nozzle exit will also be in the same order. If a more refined grid size of less than 0.125 mm is provided at the nozzle exit, it will violate the dilute approximation of Lagrangian spray modeling. It requires the volume of spray parcels to be smaller than the computational cell where the parcels are located; therefore, 0.125 mm grid size is already fine enough. However, the only limitation by doing this is at the near nozzle exit, where the size of the parcels is around 0.165 mm. For ROI-based simulations of the Spray

G injector, the specified grid size has shown promising results in the literature (Saha et al. 2016). Using such a grid resolution in the simulation using the CONVERGE code, the total number of cells obtained is in the range of 11 to 13 million. Each simulation took approximately 180 mins to finish using 144 cores on High-Performance Computing facility at IIT Delhi. **Figure 6** shows the validation for the liquid and the vapor penetrations obtained from the simulations with the ECN experimental data.

The validation studies of the Spray G injector have been performed and published by several researchers in the past (Aguerre and Nigro 2019; Manin et al. 2015; Saha et al. 2016). However, the experimental data reported lower penetration values obtained from (Manin et al. 2015), which the ECN no longer recommends. This work validates using the latest experimental data from ECN, which is higher (approx. by 10 mm at 1 ms) due to the threshold changes in the spray image processing. Moreover, most Spray G modeling studies have been carried out using the standard  $k-\epsilon$  turbulence model with tuned turbulence model constants or LES with unphysical wide (35 to 50 degrees) plume cone-angles to match the spray penetrations (Paredi et al. 2018; Saha et al. 2016; Sphicas et al. 2017). GDI spray plume cone angles are not supposed to be very wide. The RNG  $k-\epsilon$  turbulence model is recommended for engine combustion modeling because of its ability to capture the swirling flows and effect of different length scales when compared to standard  $k-\epsilon$  (Han and Reitz 1995; Kim, Song, and Park 2015). This indicates a severe flaw in the literature. The purpose of spray studies in IC engines is to facilitate combustion analysis of IC engines. However, when two different turbulence modeling approaches are adopted for reacting and non-reacting cases, then the purpose of spray modeling is not served. Nevertheless, to maintain the consistency over the turbulence models between spray and

**Figure 6.** Validation of the predictions for liquid and vapor penetrations using the simulation model setup with the latest ECN experimental data.

combustion modeling for an IC engine, as primary motive of spray studies is to help in making a better combustion model, this study is carried out using the RNG k- $\epsilon$  turbulence model to consider the effects of different length scales incorporated in the dissipation transport equation. The breakup length and breakup time constants from the KH-RT breakup length model is used to tune the simulated data to match the experimental data. The values of the breakup length constant and breakup time constant used throughout this work is 15 and 30. It has been observed from the results that up to 0.8 ms, the simulated results are shown in perfect agreement with the experimental data. Beyond 0.8 ms, the simulated values are a bit over-predicting. The actual fuel injection time of the Spray G injector is 0.78 ms. The time instant beyond the 0.78 ms is the post-injection period. The spray modeling literature generally validates the liquid and vapor penetration during the time of spray injection. However, by modeling the spray injection until 1 ms, the authors have already covered some post-injection period. The time period between 0.78 ms to 2 ms is a post-injection duration. From the experimental point of view, the purpose of performing experiments beyond the post-injection period is to understand the spray characteristics such as plume merging and plume collapse. From the modeling point of view of an IC engine simulation, the main target of a spray simulation is to validate the liquid and vapor penetration during the period of spray injection. Moreover, the way the spray penetrations are estimated in a CFD simulation, that could be easily viable for the time period during the spray injection. During the post-injection

period, the amount of liquid parcel mass left will be much less. CFD results will always indicate penetration value increasing with time, as it undertakes the smallest portion of the liquid mass into consideration for evaluating the liquid penetration. As a result, the liquid penetration in this study shown in Figure 6 is increasing in nature. It is evident from Figure 7(a,b), that majority of the spray parcels are in sub-micron level, and through experimental techniques, it is very hard to detect the presence of such small droplets.

Experimental techniques like Mie-scattering depend on the droplet size and the wavelength of the incoming light source. In order to capture the presence of the smallest droplets of the spray, the droplet size should be similar or larger than the wavelength of the incoming light source. Typical Nd: YAG laser wavelength is 532 nm, and a typical LED light source wavelength is in the range of 400–700 nm. When the droplet size is around 0.2 micron it will be difficult to detect the presence of those droplets using Mie-scattering techniques. Therefore, it would not be meaningful to compare the model predictions of the liquid or the vapor penetrations with experimental data beyond a certain time instant. Therefore, modeling the spray characteristics of different fuels till 1 ms is sufficient in this study. Moreover, the number of crank angles corresponding to 1 ms injection duration in an IC engine would be 7.2 °CA, 9 °CA, and 12 °CA for an engine running at 1200, 1500, and 2000 RPMs, respectively. Considering this simulating the spray injection for 1 ms is a sufficient duration for which validation exercise can be done. From the latest ECN data, the liquid penetration does not go till 2 ms. As mentioned

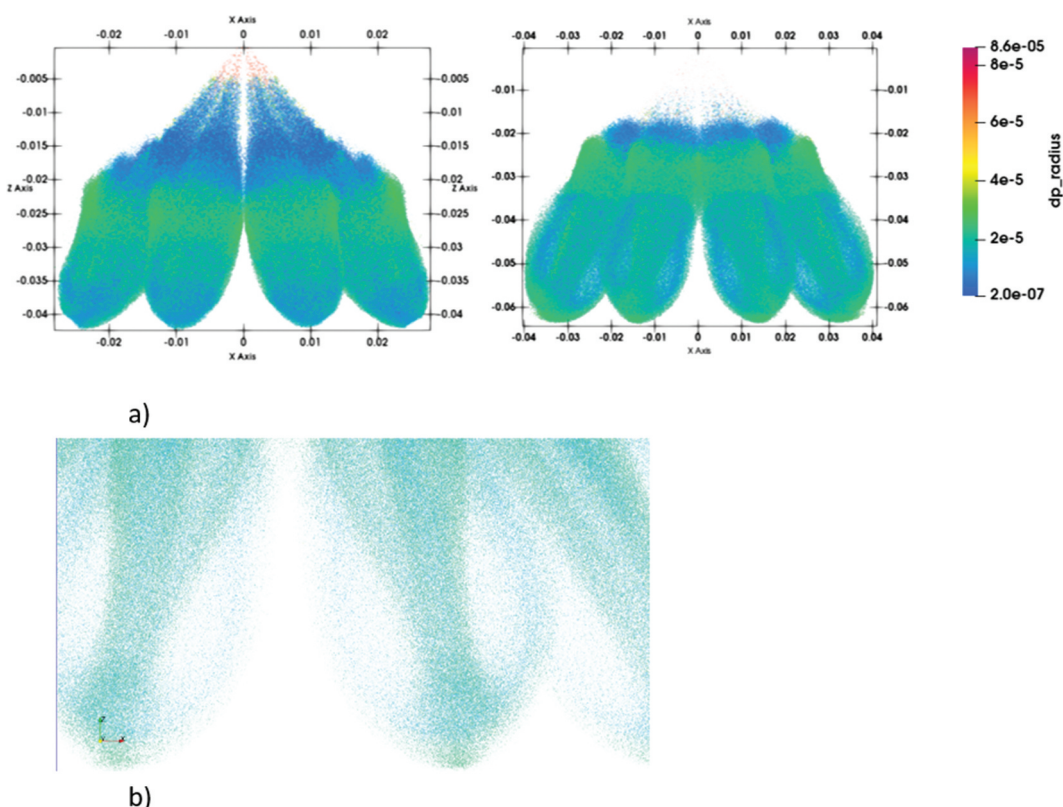


**Figure 7.** (a) Comparison of spray shape in terms of liquid droplet radius at 1 ms and 2 ms (b) enlarged view of spray plumes at 2 ms.

earlier, the previous set of ECN which went till 2 ms are no longer recommended. The latest experimental data (liquid penetration) is calculated based on 2 threshold limits (high and low threshold). The higher threshold data is coming to zero right after 1 ms (as shown in Figure 6) after the start of injection. However, the low threshold value is coming to zero at nearby 1.6 ms. The model setup which provides reasonable agreement with the latest vapor penetration data, also showed reasonable agreement with the liquid penetration data corresponding to the lower threshold values. It is seen that the maximum deviation is at 2 ms and the model is over predicting by less than 10 mm. The main aim of this study is to understand the spray behavior by using the binary and ternary blends for a GDI environment. Since the experimental data is not available for the alternative fuels, a case with iso-octane fuel is prepared and it is validated with the experimental data. The validated case setup is used for simulating the GDI sprays using the binary and ternary blended fuels, which is missing in the literature.

### 3.2. Influence of fuel properties

Unlike a conventional port fuel injector (PFI) spray, the GDI spray operates at a higher pressure and temperature range (PFI – 5 to 6 bar, GDI 150 to 200 bar (Busch et al. 2012)). The literature has observed that the fuel properties affect the spray atomization at elevated conditions (Bao

et al. 2014; Galle et al. 2013). Parametric studies using hypothetical scenarios have been carried out with the validated case setup to determine the relative importance of the different fuel properties on GDI spray characteristics. For each parametric study, the values of a specific property of iso-octane fuel varying with fuel temperature are replaced by those of ethanol, and the results obtained from those simulations are shown in Figures 8–10. Similar numerical experiments by varying physical or chemical properties elucidate dominant factor/process in a complex problem as shown in the literature (Battistoni and Grimaldi 2010; Saha, Abu-Ramadan, and Li 2013; Zhao et al. 2018). Such investigations are only possible in a numerical study and this parametric study has not been reported in the literature yet, to the best of the knowledge of the authors. Details of the cases studied in this work and the changes made are summarized in Table 5.

**Table 5.** Details of the cases performed to understand the influence of fuel properties on spray characteristics.

Case number	Details
Case 1	Iso-octane
Case 2	Ethanol
Case 3	Iso-octane with viscosity of ethanol
Case 4	Iso-octane with surface tension of ethanol
Case 5	Iso-octane with heat of vaporization of ethanol
Case 6	Iso-octane with density of ethanol

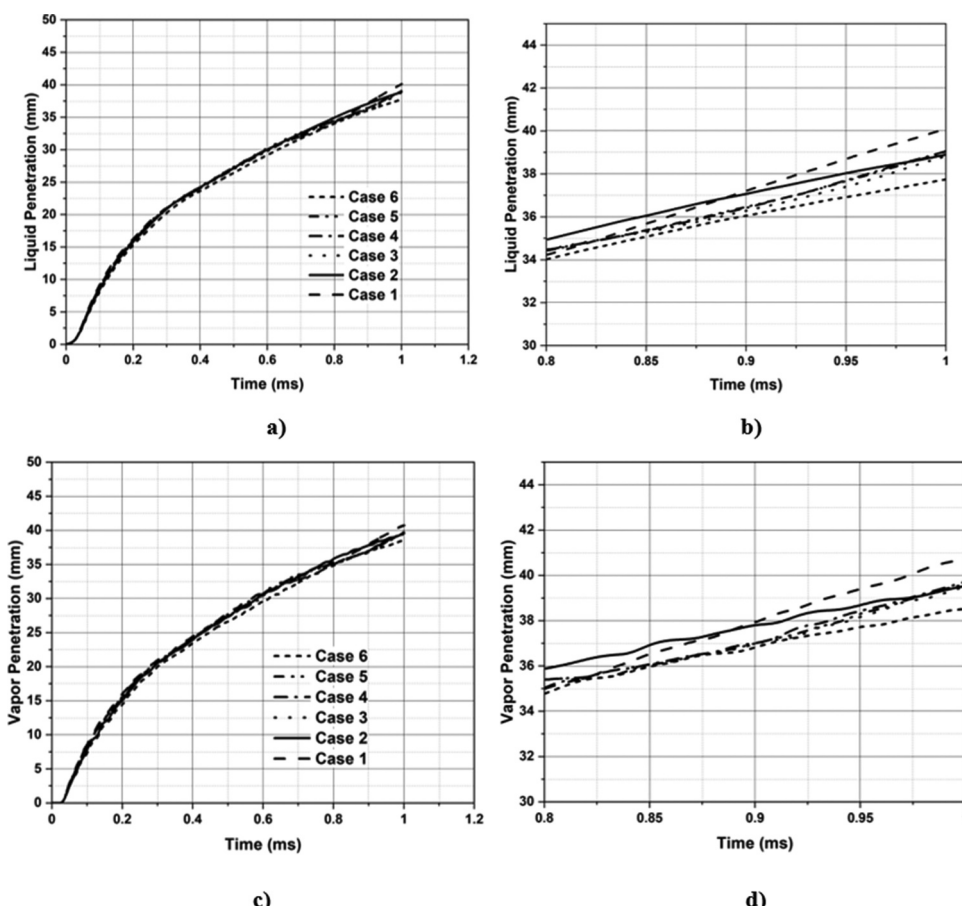


**Figure 8.** Effects of replacing the individual fuel properties of iso-octane with those of ethanol on spray penetrations: (a, c) full range data; (b, d) enlarged view from 0.8 ms to 1 ms (refer to Table 5 for case details).

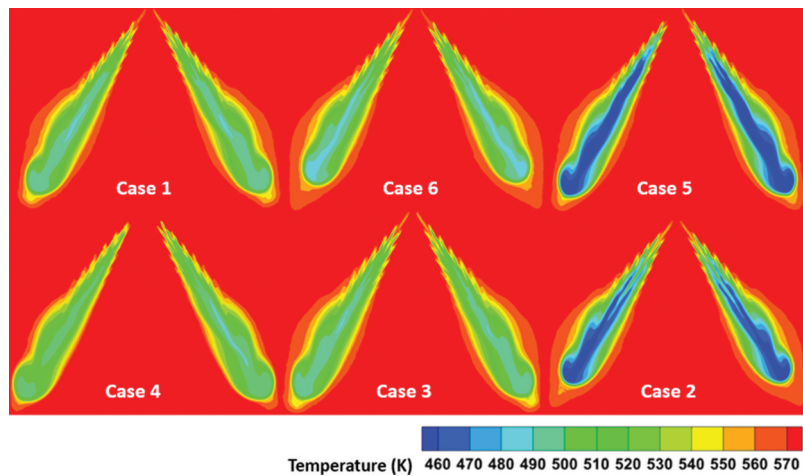


**Figure 9.** Effects of replacing the individual fuel properties of isoctane with those of ethanol on temperature contour in a vertical cut section with two diametrically opposite plumes at 0.8 ms (refer to Table 5 for case details).

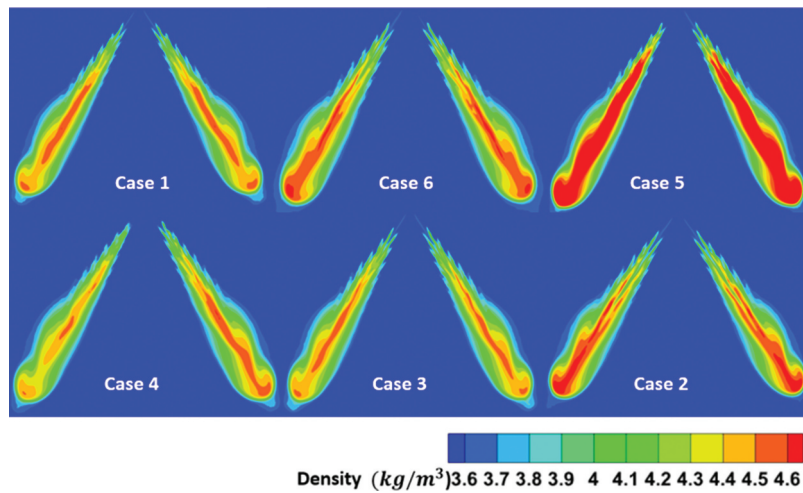


**Figure 10.** Effects of replacing the individual fuel properties of isoctane with those of ethanol on the density contours in a vertical cut section with two diametrically opposite plumes at 0.8 ms (refer to Table 5 for case details).

No significant difference is observed in the penetration results (Figure 8(a,c)) by varying the fuel properties. However, the effect of the fuel property change could be visualized from the enlarged section of penetration result

(Figure 8(b,d)), vertical cut section of two diametrically opposite plumes (Figures 9 and 10, and horizontal cut section of plumes at a distance of 15 mm from the injector location (Figure 11). Under GDI operating conditions,

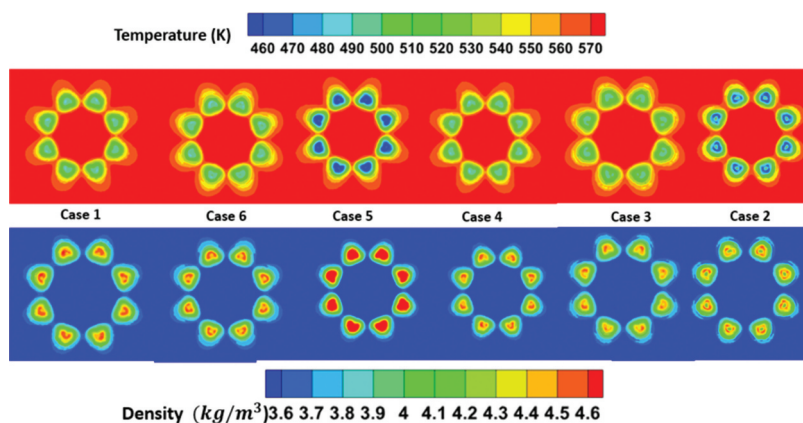


**Figure 11.** Effects of replacing the individual fuel properties of isoctane with those of ethanol on the contours of the density and temperature on a horizontal cut-plane at 15 mm downstream of the fuel injector tip at 0.8 ms (refer to Table 5 for case details).

there is a strong possibility of the plume-to-plume interaction in a multi-hole GDI injector. There are several reasons behind such a phenomenon. Firstly, at the time of injection, the droplets in a GDI system experience higher temperatures compared to PFI, which aggravates vaporization. Vapor formation leads to volume expansion of individual spray plumes, resulting in enhanced plume-to-plume interactions. Secondly, a GDI injector has much lower drill-angle (cf. Figure 2) when compared to a diesel injector. Due to this, the fuel spray vaporizes quickly, and the differences between ethanol (case 2) and isoctane (case 1) are shown in Figures 8-10. From the temperature contour results (Figures 9 and 11), not much differences in the contours are observed by the change in the fuel properties, except with case 2 and case 5, where case 2 is pure ethanol and case 5 is with ethanol heat of vaporization on an isoctane fuel. These changes are also distinguishable from density contours (case 5 and case 6) when compared with case 1 as predicted. This variation clearly indicates that the fuel properties (density and heat of vaporization) could play a vital role in blended fuels. The same is also presented in the Figure 11, indicating the charge cooling effect. More on charge cooling effect will be discussed in the next section. Surface tension is an important property which helps in understanding the breakup of a liquid droplet. Liquid droplets will encounter delay in the

breakup when the surface tension forces are dominant. The following Figure 12 shows the scattered results of liquid Weber number along the axial direction of the injector.

The nondimensional Weber number signifies the dominant force in a liquid droplet. Weber number is defined as the ratio of aerodynamical forces to the surface tension forces. The higher the surface tension forces, the slower the droplet breakup, and vice versa.

$$We = \frac{\rho v^2 d}{\sigma} \quad (i)$$

where,  $\rho$  – parcel density,  $v$  – parcel velocity,  $d$  – parcel diameter and  $\sigma$  – surface tension force. The Figure 12(a,c) represents the liquid Weber number of ethanol along the axial direction and b, d represents the same for isoctane. It is observed that in case of the isoctane the Weber number is lower (Figure 12(b,d)) compared to the case of ethanol (Figure 12(a,c)). In other way, it describes that the surface tension forces in case of isoctane are dominant in this simulation. This helps in slower the breakup of isoctane fuel droplets, and which eventually penetrates farther than the ethanol fuel droplet.

Figure 13 compares the differences in the SMD by changing the fuel properties, where it can be observed that case 5 (change in the heat of vaporization) is recorded a lower SMD than the other cases. Pure ethanol is also recorded a similar trend of

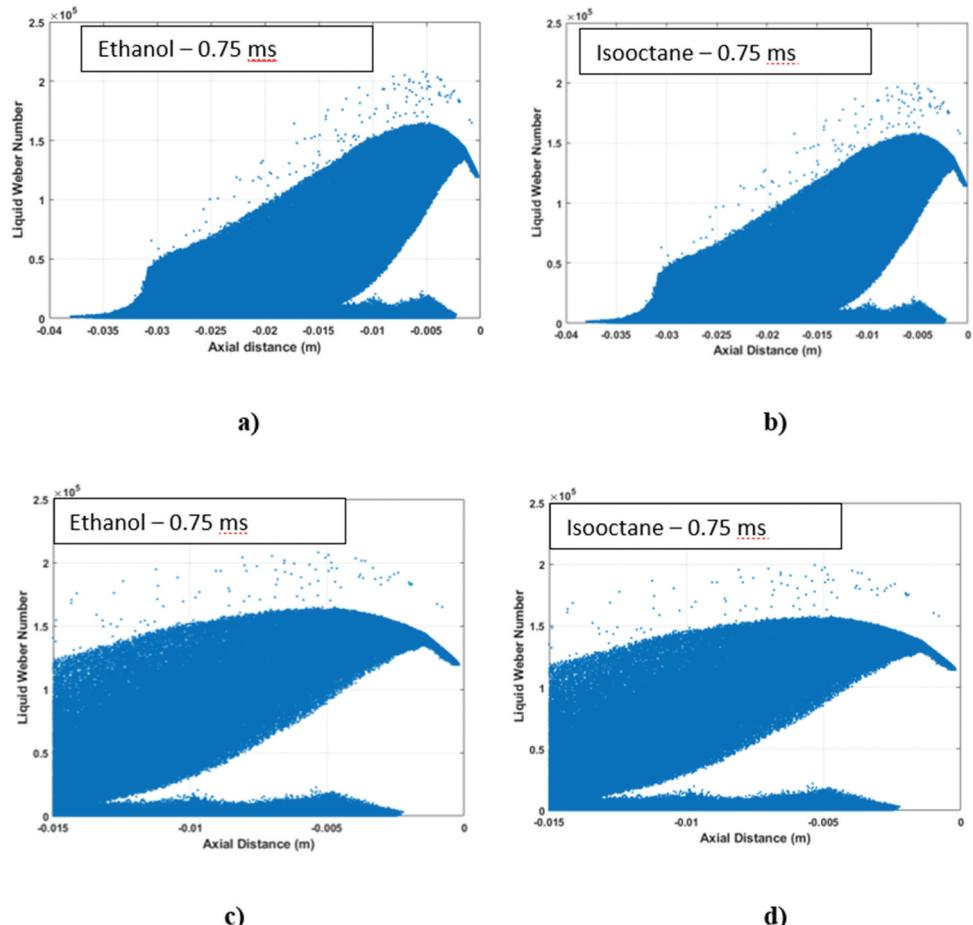


**Figure 12.** Comparison of liquid Weber numbers of the spray parcels along the axis of the injector for ethanol and isoctane (a) ethanol, (b) isoctane, (c) enlarged view for ethanol, (d) enlarged view for isoctane) at 0.75 ms of the spray injection duration.

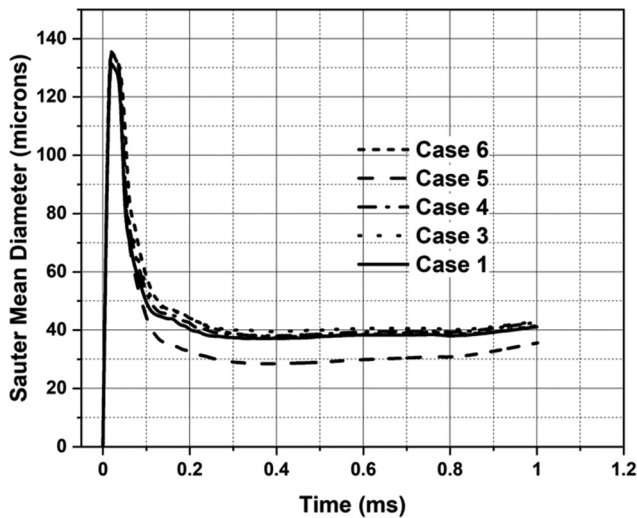


**Figure 13.** Effects of replacing the individual fuel properties of isoctane with those of ethanol on SMD variations.

SMD values, which is shown in [Figure 15](#). From the results mentioned above, it is observed that if isoctane fuel has an ethanol-like latent heat of vaporization, the spray behaves similar to the case of pure ethanol.

The viscosity of a fluid defines the measure of resistance to deformation caused by shear. As the fuel temperature increases, the viscosity of the fuel decreases linearly ([Kim et al. 2020](#)). This is because the cohesive forces are weakened. The higher the ethanol content, the higher the viscosity. The fuel property density also acts similarly. As the temperature of the fuel increases, the density of the fuel decreases. However, the density of the ethanol is higher than the isoctane, so by increasing the ethanol content in a blend, the density will also increase.

The behavior of binary and ternary blended fuels in GDI systems

Adding ethanol up to a volume percentage of 15% in a gasoline engine is accepted. It is called the octane booster, through which the engine can operate at higher compression

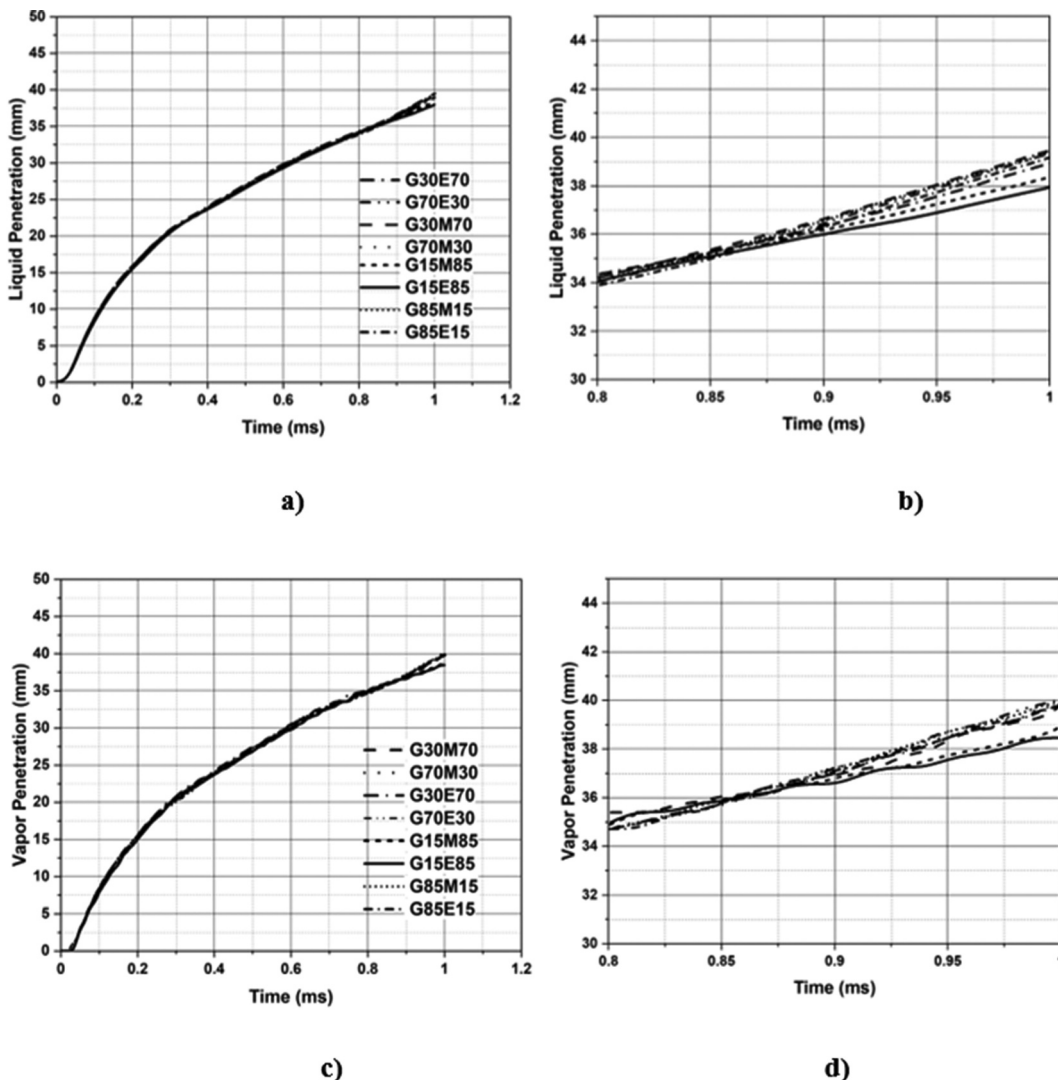


**Figure 14.** Comparison of liquid and vapor penetrations for different binary blended fuels: (a, c) liquid and vapor penetration; (b, d) enlarged view of liquid and vapor penetration from 0.8 ms to 1 ms.

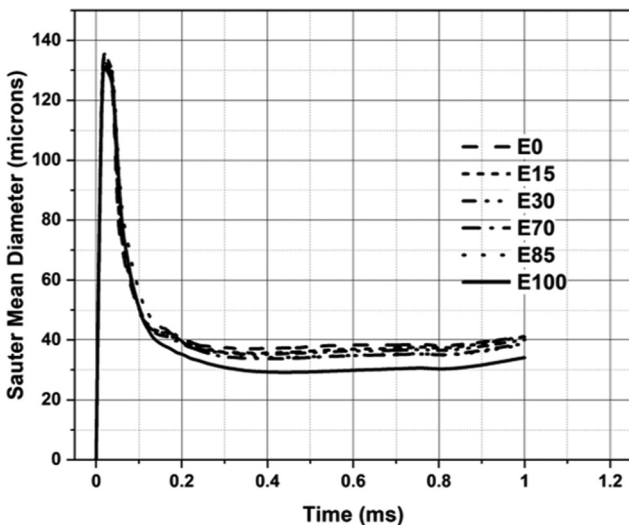


Figure 15. Sauter mean diameter (SMD) variation for different ethanol blends.

ratios without getting any trouble from the knocking. However, flex-fuel vehicles (FFV's) are such that it operates with 85% of ethanol or with complete gasoline or any other ethanol composition below 85% and gasoline, as mentioned in the previous section. Depending on the climatic conditions during the winter, the gasoline content in an FFV can increase up to 30%, which helps tackle the effects of cold start conditions.

As discussed in the previous section, methanol can be served as one of the potential alternatives to gasoline. It is known that methanol has higher viscosity and surface tension than iso-octane. The atomization characteristics are poor for the liquids having a higher viscosity. In this work, several simulations were carried out on the binary blend of methanol and iso-octane to promote methanol as an octane booster (G15M85). Several simulations were also carried by using G70M30 and G70E30 fuels by considering the winter conditions. Figure 14 shows the liquid and vapor penetration results comparison of binary blended fuels, and Figure 15 shows the SMD variation results of various ethanol blends. Figure 15 shows the footprint comparison of G15E85 and pure iso-octane fuel at various locations from the injector.

Figure 14 shows the comparison of E85 liquid and vapor penetration in the chamber with the other binary blends. The literature shows that the spray penetration increases by the gasoline content in a gasoline-ethanol blend (Gao, Jiang, and Huang 2007). A similar trend is also evident from this work, as shown in Figure 14. Increasing the ethanol content decreases the spray tip penetration, whereas the spray with higher iso-octane content increases. This helps understand that ethanol fuel has better vaporization than gasoline ones (Gao, Jiang, and Huang 2007). Several fuel properties play a role in defining the fuel spray behavior. As mentioned in the previous section, just like the spray penetration length, the spray's SMD also increases as the iso-octane content in the blend increases (shown in Figure 15), which is predicted. Figures 16 and 17 show the temperature and density contours at different downstream locations from the injector tip at 0.8 ms.

Due to latent heat difference, the local cooling of air-fuel mixtures by 30–40 K is seen from the results (Figure 16) between Isooctane and G15E85 at different positions perpendicular to the tip of the injector, through temperature contours. An approx. 10% change in local density of air-fuel mixture is also been observed in this work at the same positions, as shown in Figure 17. The higher enthalpy of vaporization increases the charge cooling effect, and it will allow an engine to run at higher compression ratios, which eventually increases the efficiency of the engine (Chen and Stone 2011). One of the significant advantages of the GDI engine over the PFI engine is the charge cooling effect. In a PFI system, the charge (mixture of fuel and air) will be introduced during the suction stroke, and at the end of the compression stroke, the temperature inside the cylinder will rise. The charge will auto-ignite and produces a knock when the temperature reaches higher than the fuel's flashpoint. However, for a GDI engine, the cooling effect of the injected spray results in lower temperature at the end of the compression stroke. It allows the engine to run at higher compression ratios (Singh 2017). Typically, it allows the GDI engine to operate at slightly higher compression ratios than PFI engines (Anderson et al. 1996; Golzari, Li, and Zhao 2016; Oh et al. 2010; Wyszynski, Stone, and Kalghatgi 2002; Zhao, Lai, and Harrington 1999). This suggests that binary or

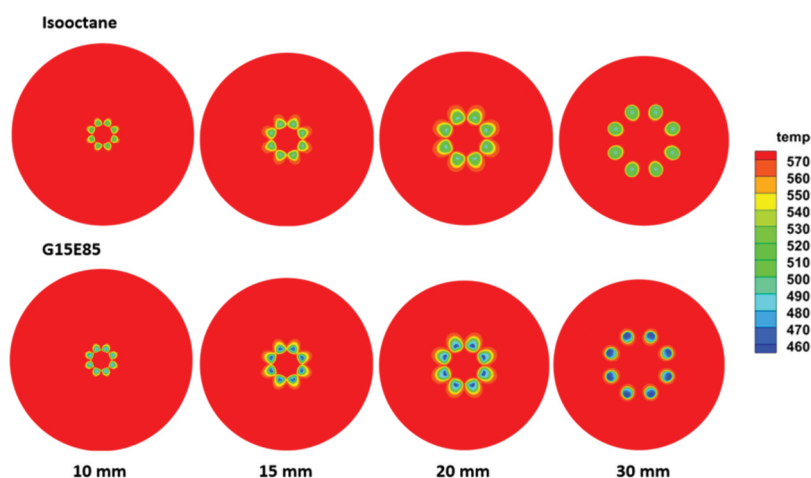
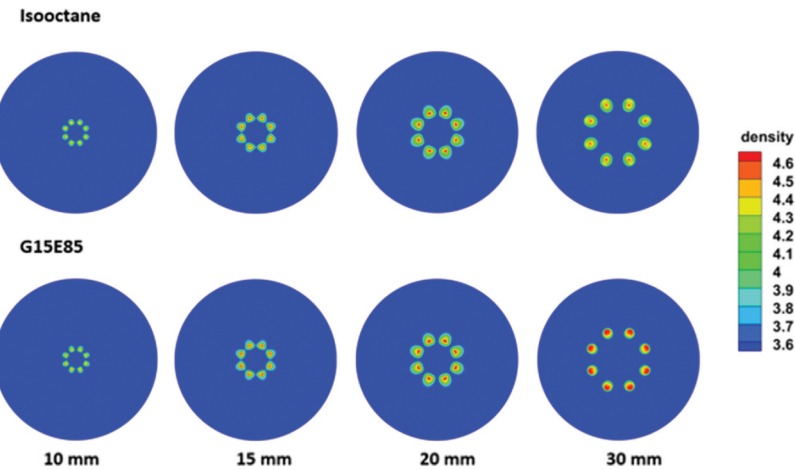
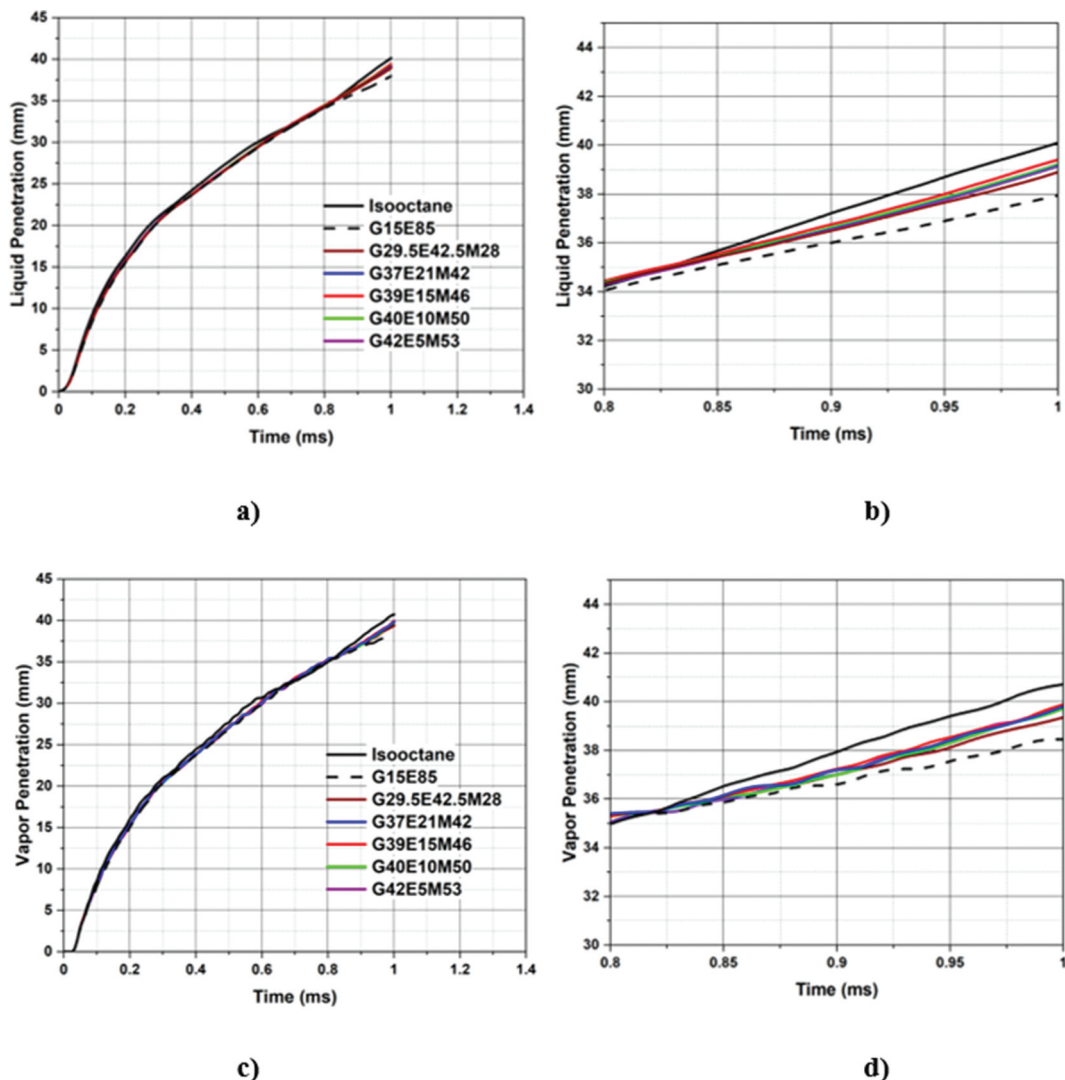


Figure 16. Temperature (K) contours at different downstream locations from the injector tip at 0.8 ms for iso-octane and G15E85 blend.



**Figure 17.** Density ( $\text{kg}/\text{m}^3$ ) contours at different downstream locations from the injector tip at 0.8 ms for isoctane and G15E85 blend.



**Figure 18.** Comparison of liquid and vapor penetrations for different GEM blends: (a, c) liquid and vapor penetration; (b, d) enlarged view of liquid and vapor penetration from 0.8 ms to 1 ms.

ternary blended fuels (gasoline with ethanol and methanol) will help run the GDI engines even at higher compression ratios, and better performance can be achieved.

The following correlations represent important spray characteristics like penetration and breakup length (Subramanian 2017).

$$S = 3.07 \left( \frac{P_{inj}}{\rho_g} \right)^{\frac{1}{4}} (Dt)^{\frac{1}{2}} \left( \frac{294}{T_g} \right)^{\frac{1}{4}} \quad (\text{ii})$$

Where,  $P_{inj}$  – Pressure drop across the injector,  $\rho_g$  – gas density,  $D$  – Nozzle hole diameter,  $t$  – time,  $T_g$  – gas temperature

$$L_b = 15.8 \left( \frac{\rho_f}{\rho_a} \right)^{0.5} D \quad (\text{iii})$$

$\rho_f$  – Density of the fuel,  $\rho_a$  – Density of the air,  $D$  – Nozzle hole diameter

From the above corelations (Equations ii and iii), it is evident the spray characteristics may not considerably change due to change in fuel for a given operating conditions. Therefore, the findings from this study should be considered reasonable.

As mentioned in the previous sections, the ternary blend's primary motive is to replace some ethanol with methanol fuel without hampering the performance. Similar work has been reported in the literature (Turner et al. 2012, 2013), but with PFI engines. The nozzle geometry and operating conditions are different for the PFI and GDI systems. Hence, this work is investigating the behavior of sprays with GEM fuels in case of a typical GDI injector. The liquid and vapor penetration of the various GEM blends are shown in Figure 18.

It is observed from Figure 18, that the isoctane fuel has higher penetration lengths than the binary and ternary blended fuels. This is expected because of the higher temperature of the ambient gas in the constant volume chamber, which would decrease the fuel density and eventually help in attaining higher injection velocity for a fixed pressure drop across the nozzle (Bao et al. 2014).

It is feasible to have blends of gasoline, ethanol and methanol. A difference of 2 to 3 mm has been observed in the penetration results between the isoctane and E85 fuel, and it elucidates the influence of isoctane concentration in the E85 blend. The data shows that all GEM blends' penetration resembles similar to each other, and their penetration distance lies between the isoctane and E85, respectively. Through the enlarged view of penetration results (Figure 17(b,d)), it is observed that by increasing the isoctane content in the blend, the penetration length is increasing. The same is observed in the case of binary blends as well (Figure 13). From this work it also observed that there is no significant change in the penetration results by replacing the ethanol with methanol.

Nevertheless, this variation could be because all the blends are formulated so that the fluid properties resemble the same as E85 fuel. It indicates that some ethanol can be replaced with methanol for a GDI-based FFV to reduce the overall utilization of the ethanol fuel. This will be helpful in nations where the ethanol production cost is higher than methanol.

#### 4. Conclusions

The present study is carried out on an eight-hole counter bored GDI fuel injector from the ECN. The standard ROI-based blob injection approach is adopted in this work, and the RNG k- $\epsilon$  turbulence model is used to account for spray induced turbulence. The key points taken from the current study are summarized below:

- This work proposes a spray modeling approach for GDI systems, validated with the latest experimental data on liquid and vapor penetration from ECN, which is higher than the previously used ECN data by the spray modeling community, due to the threshold change in spray image processing, without tuning the turbulence model constants of standard k- $\epsilon$  model or assuming unphysical wide plume cone angle. The breakup length and breakup time constants from the KH-RT breakup length model were used as tuning parameters to match the experimental data. The simulated results of isoctane have shown reasonable agreement with the experimental data. A similar case setup is used for the rest of all simulations carried on binary and ternary blended fuels.
- Parametric studies have been carried out to understand the relative importance of fuel properties. In each simulation, one of the isoctane fuel properties was replaced with that of ethanol to find the influence of that specific fuel property on spray characteristics. As expected, the fuel properties, such as density and heat of vaporization, showed differences in the penetration results and the density and temperature contours. It has been observed that the surface tension forces are dominant in isoctane compared with ethanol, and it allows the isoctane fuel to break up slower and penetrate farther. Thus, the isoctane fuel has the farthest penetration length compared with alcoholic fuels and blends. From the SMD results, it has also been observed that if isoctane fuel has an ethanol-like latent heat of vaporization, the spray behaves similar to the case of pure ethanol.
- Ethanol has a lower boiling point temperature than isoctane, enabling the ethanol liquid fuel to vaporize quickly. Nevertheless, the heat of vaporization is higher in ethanol than isoctane, which indicates that ethanol requires more energy to convert the liquid fuel into vapor. This work shows differences in penetration lengths and SMD with increased isoctane content in a binary blend. The increase in isoctane content in a binary blend has shown an increase in penetration length of approx. 2 mm compared with E85 with E15 fuel. The SMD of approx. 8-micron difference has been observed between E0 and E100 for the same operating conditions; a similar trend has also been seen in the literature.
- Alcohol fuels have a higher enthalpy of vaporization, which increases the charge cooling effect. As expected, using an alcohol-based blend in a GDI system, a local cooling of air-fuel mixture by 30-40 K and a 10% change in local density of air-fuel mixture has been observed in this work. This charge-cooling effect will allow an engine



to run at even higher compression ratios, eventually increasing its efficiency, negating the lower calorific value for an alcohol-based fuel.

- The influence of isoctane on an E85 blended fuel has shown a difference of approx. 2 to 3 mm in penetration length between isoctane and E85. GEM blends used in this work showed similar performance, and no significant differences have been observed when part of ethanol concentration is replaced with the methanol ones. Indicating that GEM blends can be used in a GDI-based FFV, and the ethanol concentration can be replaced with some amount methanol, maintaining the AFR as with E85 fuel, in such nations where the production of ethanol is costlier than methanol.

## Nomenclature

$h_{fg}$	Latent heat of vaporization
$k$	Turbulence kinetic energy
$\varepsilon$	Turbulent dissipation rate
GDI	Gasoline Direct Injection
PFI	Port Fuel Injection
ECN	Engine Combustion Network
DPM	Discrete Phase Modeling
URANS	Unsteady Reynolds-Averaged Navier-Stokes
RNG	Renormalization Group
FFV	Flex-Fuel Vehicle
ICEV	Internal Combustion Engine Vehicle
BEV	Battery Electric Vehicle
LCA	Life Cycle Analysis
GWP	Global Warming Potential
PHEV	Plug-in Hybrid Electric Vehicle
FHEV	Full Hybrid Electric Vehicle
STP	Standard Temperature and Pressure
AFR	Air-Fuel Ratio
RON	Research Octane Number
EU	European Union
RED	Renewable Energy Directive
EPA	Environmental Protection Agency
NITI Aayog	National Institution for Transforming India Aayog
GEM	Gasoline-Ethanol-Methanol
CFD	Computational Fluid Dynamics
CFL	Courant-Freidrichs-Lewy
ROI	Rate of Injection
PISO	Pressure Implicit with Splitting of Operators
SI	Spark Ignited
CVC	Constant Volume Chamber
KH	Kelvin-Helmholtz
RT	Rayleigh-Taylor
NTC	No Time Counter
NIST	National Institute of Standards and Technology
REFPROP	Reference Fluid Thermodynamic and Transport Properties
SMD	Sauter Mean Diameter
We	Weber Number
$\rho$	Parcel Density
$v^2$	Parcel Velocity
$d$	Parcel Diameter
$\sigma$	Surface Tension

## Acknowledgments

The authors thank the Science and Engineering Research Board (SERB) of the Department of Science and Technology (DST) for funding through the Early Career Research Award (ECRA) – ECR/2018/002372. The authors

thank IIT Delhi HPC facility and Dr. Manish Agarwal for computational resources and Convergent Science India for their support in our work.

## Disclosure statement

No potential conflict of interest was reported by the author(s).

## Funding

The work was supported by the Science and Engineering Research Board [ECR/2018/002372]

## References

- Aditiya, H. B., T. M. I. Mahlia, W. T. Chong, H. Nur, and A. H. Sebayang. 2016. Second generation bioethanol production: A critical review. *Renewable and Sustainable Energy Reviews* 66:631–653. doi:[10.1016/j.rser.2016.07.015](https://doi.org/10.1016/j.rser.2016.07.015).
- Aguerre, H. J., and N. M. Nigro. 2019. Implementation and validation of a Lagrangian spray model using experimental data of the ECN Spray G injector. *Computers & Fluids* 190:30–48. doi:[10.1016/j.compfluid.2019.06.004](https://doi.org/10.1016/j.compfluid.2019.06.004).
- Allocca, L., L. Bartolucci, S. Cordiner, M. Lazzaro, A. Montanaro, V. Mulone and V. Rocco. 2018. ECN Spray G injector: Assessment of numerical modeling accuracy (No. 2018-01-0306). SAE Technical Paper.
- Alternative Fuels Data Center: Ethanol Benefits and Considerations. Accessed October 12, 2021. [https://afdc.energy.gov/fuels/ethanol\\_benefits.html](https://afdc.energy.gov/fuels/ethanol_benefits.html)
- Anderson, R. W., J. Yang, D. D. Brelob, J. K. Vallance, and R. M. Whiteaker. 1996. Understanding the thermodynamics of direct injection spark ignition (DISI) combustion systems: An analytical and experimental investigation. *SAE Transactions* 2195–2204. <https://doi.org/10.4271/962018>.
- Bao, Y., Q. N. Chan, S. Kook and E. Hawkes. 2014. A comparative analysis on the spray penetration of ethanol, gasoline and isoctane fuel in a spark-ignition direct-injection engine (No. 2014-01-1413). SAE Technical Paper.
- Battistoni, M., and C. N. Grimaldi. 2010. Analysis of transient cavitating flows in diesel injectors using diesel and biodiesel fuels. *SAE International Journal of Fuels and Lubricants* 3 (2):879–900. doi:[10.4271/2010-01-2245](https://doi.org/10.4271/2010-01-2245).
- Busch, R., J. Hammer, R. Herynek, and K. Wehmeier. 2012. Advanced fuel metering gasoline-requirements and Bosch system solutions. In *Fuel systems for IC engines*, 77–85. 978-0-85709-210-6. Sawston, United Kingdom: Woodhead Publishing.
- Carsten, B. 2006. Modern concepts. *Mixture Formation in Internal Combustion Engine* Heat, Mass Transfer book series (HMT). (Berlin, Heidelberg: Springer). 225–286.
- Chen, L., and R. Stone. 2011. Measurement of enthalpies of vaporization of isoctane and ethanol blends and their effects on PM emissions from a GDI engine. *Energy & Fuels* 25 (3):1254–59. doi:[10.1021/ef1015796](https://doi.org/10.1021/ef1015796).
- Cordier, M., L. Itani, and G. Bruneaux. 2020. Quantitative measurements of preferential evaporation effects of multicomponent gasoline fuel sprays at ECN Spray G conditions. *International Journal of Engine Research* 21 (1):185–98. doi:[10.1177/1468087419838391](https://doi.org/10.1177/1468087419838391).
- Duke, D. J., C. E. Finney, A. Kastengren, K. Matusik, N. Sovis, L. Santodonato, H. Bilheux, D. Schmidt, C. Powell, and T. Toops. 2017a. High-Resolution x-ray and neutron computed tomography of an engine combustion network spray G gasoline injector. *SAE International Journal of Fuels and Lubricants* 10 (2):328–43. doi:[10.4271/2017-01-0824](https://doi.org/10.4271/2017-01-0824).
- Duke, D. J., A. L. Kastengren, K. E. Matusik, A. B. Swantek, C. F. Powell, R. Payri, D. Vaquerizo, L. Itani, G. Bruneaux, R. O. Grover Jr, et al. 2017b. Internal and near nozzle measurements of engine combustion network “Spray G” gasoline direct injectors. *Experimental Thermal and Fluid Science* 88:608–21. doi:[10.1016/j.expthermflusci.2017.07.015](https://doi.org/10.1016/j.expthermflusci.2017.07.015).

- European Union. 2009. Directive 2009/28/EC of the European parliament and of the council of 23 April 2009 on the promotion of the use of energy from renewable sources and amending and subsequently repealing directives 2001/77/EC and 2003/30/EC. *Official Journal of the European Union* 5: 2009.
- Galle, J., S. Defruct, C. Van de Maele, R. P. Rodriguez, Q. Denon, A. Verliefde, and S. Verhelst. 2013. Experimental investigation concerning the influence of fuel type and properties on the injection and atomization of liquid biofuels in an optical combustion chamber. *Biomass and Bioenergy* 57:215–28. doi:10.1016/j.biombioe.2013.07.004.
- Gao, J., D. Jiang, and Z. Huang. 2007. Spray properties of alternative fuels: A comparative analysis of ethanol-gasoline blends and gasoline. *Fuel* 86 (10–11):1645–50. doi:10.1016/j.fuel.2006.11.013.
- Golzari, R., Y. Li and H. Zhao. 2016. Impact of port fuel injection and in-cylinder fuel injection strategies on gasoline engine emissions and fuel economy (No. 2016-01-2174). SAE Technical Paper.
- Gutierrez, L., A. B. Mansfield, M. Fatouraie, D. Assanis, R. Singh, J. Lacey, M. Bear and M. Wooldridge. 2018. Effects of engine speed on spray behaviors of the engine combustion network “Spray G” gasoline injector (No. 2018-01-0305). SAE Technical Paper.
- Han, Z., and R. D. Reitz. 1995. Turbulence modeling of internal combustion engines using RNG  $\kappa$ - $\epsilon$  models. *Combustion Science and Technology* 106 (4–6):267–95. doi:10.1080/00102209508907782.
- H.R.6 - 110th Congress (2007-2008): Energy Independence and Security Act of 2007 | Congress.gov | Library of Congress. Accessed October 10, 2021. <https://www.congress.gov/bill/110th-congress/house-bill/6>
- Jin, D., K. Choi, C. L. Myung, Y. Lim, J. Lee, and S. Park. 2017. The impact of various ethanol-gasoline blends on particulates and unregulated gaseous emissions characteristics from a spark ignition direct injection (SIDI) passenger vehicle. *Fuel* 209:702–12. doi:10.1016/j.fuel.2017.08.063.
- Kim, Y., W. Kim, S. Baek, and K. Lee. 2020. Experimental study on the Spray characteristics of ethanol gasoline blended fuel in a direct injection system. *International Journal of Automotive Technology* 21 (3):555–61. doi:10.1007/s12239-020-0052-5.
- Kim, T., J. Song, and S. Park. 2015. Effects of turbulence enhancement on combustion process using a double injection strategy in direct-injection spark-ignition (DISI) gasoline engines. *International Journal of Heat and Fluid Flow* 56:124–36. doi:10.1016/j.ijheatfluidflow.2015.07.013.
- Liu, W., Y. Lu, Y. Kang, J. Yan, and C. F. Lee. 2021. Macroscopic characteristics of flash-boiling spray focused on plume interaction. *International Journal of Heat and Mass Transfer* 170:120999. doi:10.1016/j.ijheatmasstransfer.2021.120999.
- Manin, J., Y. Jung, S. A. Skeen, L. M. Pickett, S. E. Parrish and L. Markle. 2015. Experimental characterization of DI gasoline injection processes (No. 2015-01-1894). SAE Technical Paper.
- Methanol Economy | NITI Aayog. Accessed October 10, 2021. <https://www.niti.gov.in/methanol-economy>.
- Ministry of Petroleum and Natural Gas Economic & Statistics Division. Indian Petroleum & Natural Gas Statistics 2019-20. Accessed January 19, 2022. <https://mopng.gov.in/flipbook/2020/index.html>
- Mohapatra, C. K., D. P. Schmidt, B. A. Sforozzo, K. E. Matusik, Z. Yue, C. F. Powell, S. Som, B. Mohan, H. G. Im, J. Badra, et al. 2020. Collaborative investigation of the internal flow and near-nozzle flow of an eight-hole gasoline injector (Engine Combustion Network Spray G). *International Journal of Engine Research* 1468087420918449. doi:10.1177/1468087420918449.
- Oh, S., S. Lee, Y. Choi, K. Y. Kang, J. Cho and K. Cha. 2010. Combustion and emission characteristics in a direct injection LPG/gasoline spark ignition engine (No. 2010-01-1461). SAE Technical Paper.
- Paredi, D., T. Lucchini, G. D’-Errico, A. Onorati, A. Montanaro, L. Allocata and R. Ianniello. 2018. Combined experimental and numerical investigation of the ECN Spray G under different engine-like conditions. In 2018 SAE World Congress Experience, WCX 2018 Detroit, Michigan, USA (Vol. 2018, pp. 1–15). SAE International.
- Paredi, D., T. Lucchini, G. D’-Errico, A. Onorati, L. Pickett, and J. Lacey. 2020. Validation of a comprehensive computational fluid dynamics methodology to predict the direct injection process of gasoline sprays using Spray G experimental data. *International Journal of Engine Research* 21 (1):199–216. doi:10.1177/1468087419868020.
- Payri, R., F. J. Salvador, P. Martí-Aldaraví, and D. Vaquerizo. 2017. ECN Spray G external spray visualization and spray collapse description through penetration and morphology analysis. *Applied Thermal Engineering* 112:304–16. doi:10.1016/j.applthermaleng.2016.10.023.
- Piazzullo, D., M. Costa, L. Allocata, A. Montanaro, and V. Rocco. 2017. A 3D CFD simulation of GDI sprays accounting for heat transfer effects on wallfilm formation. *SAE International Journal of Engines* 10 (4):2166–75. doi:10.4271/2017-24-0041.
- Price, P., B. Twiney, R. Stone, K. Kar and H. Walmsley. 2007. Particulate and hydrocarbon emissions from a spray guided direct injection spark ignition engine with oxygenate fuel blends (No. 2007-01-0472). SAE Technical Paper.
- Publications Office of the EU. n.d. Determining the environmental impacts of conventional and alternatively fuelled vehicles through LCA. Accessed November 1, 2021. <https://op.europa.eu/en/publication-detail/-/publication/1f494180-bc0e-11ea-811c-01aa75ed71a1>
- Reitz, R. D. 1987. Modeling atomization processes in high-pressure vaporizing sprays. *Atomisation Spray Technology* 3 (4):309–37.
- Richards, K. J., P. K. Senecal, and Pomraning E. 2021. CONVERGE 2.4, convergent science. Madison, WI: Convergent Science.
- Safe Handling | METHANOL INSTITUTE. Accessed October 16, 2021. <https://www.methanol.org/safe-handling/>
- Saha, K., E. Abu-Ramadan, and X. Li. 2013. Modified single-fluid cavitation model for pure diesel and biodiesel fuels in direct injection fuel injectors. *Journal of Engineering for Gas Turbines and Power* 135 (6). doi:10.1115/1.4023464.
- Saha, K., S. Quan, M. Battistoni, S. Som, P. K. Senecal and E. Pomraning. 2017. Coupled Eulerian internal nozzle flow and Lagrangian spray simulations for GDI systems (No. 2017-01-0834). SAE Technical Paper.
- Saha, K., S. Som, M. Battistoni, Y. Li, S. Quan, and P. Kelly Senecal. 2016. Modeling of internal and near-nozzle flow for a gasoline direct injection fuel injector. *Journal of Energy Resources Technology* 138 (5). doi:10.1115/1.4032979.
- Schmidt, D. P., and C. J. Rutland. 2000. A new droplet collision algorithm. *Journal of Computational Physics* 164 (1):62–80. doi:10.1006/jcph.2000.6568.
- Senecal, K., and F. Leach. 2021. Racing toward zero: The untold story of driving green.
- Singh, S. 2017. Comparison of Fuel Economy and Gaseous Emissions of Gas-Direct Injection versus Port-Fuel Injection Light Duty Vehicles Based on Real-World Measurements.
- Sphicas, P., L. M. Pickett, S. Skeen, J. Frank, T. Lucchini, D. Sinoir, G. D’-Errico, K. Saha, and S. Som. 2017. A comparison of experimental and modeled velocity in gasoline direct-injection sprays with plume interaction and collapse. *SAE International Journal of Fuels and Lubricants* 10 (1):184–201. doi:10.4271/2017-01-0837.
- ‘Spray G’ Operating Condition – Engine Combustion Network. Accessed October 16, 2021. <https://ecn.sandia.gov/gasoline-spray-combustion/target-condition/spray-g-operating-condition/>
- Subramanian, K. A. 2017. *Biofueled reciprocating internal combustion engines*. New York: CRC Press.
- Turner, J. W., A. G. Lewis, S. Akehurst, C. J. Brace, S. Verhelst, J. Vancoillie, L. Sileghem, F. Leach, and P. P. Edwards. 2018. Alcohol fuels for spark-ignition engines: Performance, efficiency and emission effects at mid to high blend rates for binary mixtures and pure components. *Proceedings of the Institution of Mechanical Engineers, Part D: Journal of Automobile Engineering* 232 (1):36–56.
- Turner, J. W., R. J. Pearson, A. Bell, S. de Goede, and C. Woolard. 2012. Iso-Stoichiometric ternary blends of gasoline, ethanol and methanol: Investigations into exhaust emissions, blend properties and octane numbers. *SAE International Journal of Fuels and Lubricants* 5 (3):945–67. doi:10.4271/2012-01-1586.
- Turner, J. W. G., R. J. Pearson, E. Dekker, B. Iosefa, K. Johansson, and K. Ac Bergström. 2013. Extending the role of alcohols as transport fuels using iso-stoichiometric ternary blends of gasoline, ethanol and methanol. *Applied Energy* 102:72–86. doi:10.1016/j.apenergy.2012.07.044.

- Turner, J., R. Pearson, R. Purvis, E. Dekker, K. Johansson and K. Ac Bergström. 2011. GEM ternary blends: Removing the biomass limit by using iso-stoichiometric mixtures of gasoline, ethanol and methanol (No. 2011-24-0113). SAE Technical Paper.
- Verhelst, S., J. W. Turner, L. Sileghem, and J. Vancoillie. 2019. Methanol as a fuel for internal combustion engines. *Progress in Energy and Combustion Science* 70:43–88. doi:[10.1016/j.pecs.2018.10.001](https://doi.org/10.1016/j.pecs.2018.10.001).
- Verhelst, S., and T. Wallner. 2009. Hydrogen-Fueled internal combustion engines. *Progress in Energy and Combustion Science* 35 (6):490–527. doi:[10.1016/j.pecs.2009.08.001](https://doi.org/10.1016/j.pecs.2009.08.001).
- Wyszynski, L. P., C. R. Stone and G. T. Kalghatgi. 2002. The volumetric efficiency of direct and port injection gasoline engines with different fuels (No. 2002-01-0839). SAE Technical Paper.
- Yates, A., A. Bell, and A. Swarts. 2010. Insights relating to the autoignition characteristics of alcohol fuels. *Fuel* 89 (1):83–93. doi:[10.1016/j.fuel.2009.06.037](https://doi.org/10.1016/j.fuel.2009.06.037).
- Yue, Z., M. Battistoni and S. Som. 2018. A numerical study on spray characteristics at start of injection for gasoline direct injection. arXiv preprint arXiv:1810.03288.
- Zhao, F. Q., M. C. Lai, and D. L. Harrington. 1997. A review of mixture preparation and combustion control strategies for spark-ignited direct-injection gasoline engines. *SAE Transactions* 861–904. doi:[10.4271/970627](https://doi.org/10.4271/970627).
- Zhao, F., M. C. Lai, and D. L. Harrington. 1999. Automotive spark-ignited direct-injection gasoline engines. *Progress in Energy and Combustion Science* 25 (5):437–562. doi:[10.1016/S0360-1285\(99\)00004-0](https://doi.org/10.1016/S0360-1285(99)00004-0).
- Zhao, L., A. A. Moiz, S. Som, N. Fogla, M. Bybee, S. Wahiduzzaman, M. Mirzaeian, F. Millo, and J. Kodavasal. 2018. Examining the role of flame topologies and in-cylinder flow fields on cyclic variability in spark-ignited engines using large-eddy simulation. *International Journal of Engine Research* 19 (8):886–904. doi:[10.1177/1468087417732447](https://doi.org/10.1177/1468087417732447).